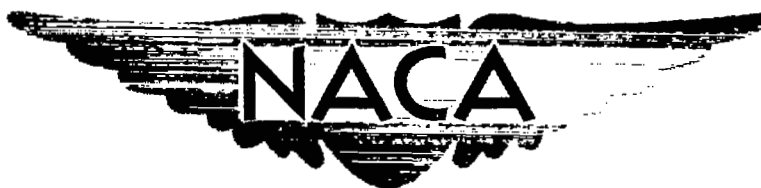


CONFIDENTIAL

Copy
RM E53A16

6

MAR 18 1953



RESEARCH MEMORANDUM

INVESTIGATION OF DISTRIBUTION OF LOSSES IN

A CONSERVATIVELY DESIGNED TURBINE

By Rose L. Whitney, Jack A. Heller, and Cavour H. Hauser

Lewis Flight Propulsion Laboratory
Cleveland, Ohio

CLASSIFICATION CHANGED

To UNCLASSIFIEDBy authority of NACA Res. Lab. Date 2-15-57
77B 3-13-57

CLASSIFIED DOCUMENT

This material contains information affecting the National Defense of the United States within the meaning of the espionage laws, Title 18, U.S.C., Secs. 793 and 794, the transmission or revelation of which in any manner to an unauthorized person is prohibited by law.

NATIONAL ADVISORY COMMITTEE
FOR AERONAUTICS

WASHINGTON

March 16, 1953

NACA LIBRARY

LANGLEY AERONAUTICAL LABORATORY
Langley Field, Va.

CONFIDENTIAL

NACA RM E53A16

NATIONAL ADVISORY COMMITTEE FOR AERONAUTICS

RESEARCH MEMORANDUM

INVESTIGATION OF DISTRIBUTION OF LOSSES IN

A CONSERVATIVELY DESIGNED TURBINE

By Rose L. Whitney, Jack A. Heller, and Cavour H. Hauser

SUMMARY

A primary objective of turbine research is to obtain information that will aid in the design of gas turbines for any given application with minimum losses. As part of a program to obtain such information, flow surveys downstream of both the stator and the rotor of an experimental turbine were made in order to obtain detailed information about the flow conditions and the losses within the machine. The single-stage, low-radius-ratio turbine studied is relatively conservative in design, having low rotor-inlet relative Mach number, low turning angle, and high reaction at the rotor-root section. Surveys of the flow conditions and of the losses within the turbine are presented. The measured over-all losses are analyzed in order to approximate the magnitudes of the various components of loss.

It was found that the major losses in the turbine were in the rotor near the blade extremities. The losses in the tip region were considerably greater than those near the hub. The existence of secondary flows at the exit of both the stator and the rotor was indicated by the presence of low-velocity cores near both the hub and the tip sections. Analysis of the losses by an empirical method indicated that the rotor-profile and the tip-clearance losses are 31 and 9 percent of the adjusted measured total rotor loss, respectively. The remaining 60 percent loss was attributed to secondary flows.

INTRODUCTION

One of the primary objectives of turbine research is to obtain information that will make possible the design of gas turbines for any given application with minimum losses. Detailed knowledge of the source, the location, and the magnitude of the losses is essential in the attainment of this objective. As part of a research program aimed at obtaining this information, surveys of the flow conditions and the losses downstream of both the stator and the rotor were made in an experimental turbine.

These surveys were made in a single-stage low-radius-ratio turbine of conservative design, having low rotor-inlet relative Mach numbers, low turning angles, and relatively high reaction at the rotor-root section.

The over-all performance of this turbine is presented in reference 1 for four rotor-blade solidities. The highest efficiency (0.89) was obtained with the 44-blade rotor, and the survey results presented herein were obtained at the design operating point for this configuration.

The results of the surveys of the flow conditions within a turbine can be interpreted directly to obtain the over-all losses downstream of each blade row. However, in order to break down the total measured loss into the individual losses caused by the blade-profile boundary layer, the secondary flows, and the tip clearance, additional information is required. A method for calculating the profile loss for conventional turbine blading, based on two-dimensional cascade data, is presented in reference 2. Coefficients, based on a number of turbine investigations, are also given in reference 2 for approximating the losses caused by secondary flows and tip clearance. As an initial attempt to analyze the over-all measured losses from the flow surveys in a given turbine, the data given in reference 2 were used to differentiate between the various sources of loss in the machine.

In this investigation, conducted at the NACA Lewis laboratory, the radial distribution of the flow and the losses within the turbine configuration were studied. In addition, the over-all measured losses were analyzed in order to determine the approximate magnitudes of the various components of the losses.

SYMBOLS

The following symbols are used in this report:

a_{cr}	critical velocity of sound, $\sqrt{\left(\frac{2\gamma}{\gamma+1}\right) gRT'}$, ft/sec
c_p	specific heat at constant pressure, Btu/(lb)(°F)
g	acceleration due to gravity, ft/sec ²
J	mechanical equivalent of heat, ft-lb/Btu
L	loss, Btu/lb
p	absolute pressure, lb/sq ft
R	gas constant, ft-lb/(lb)(°R)
r	radius, in.
s	specific entropy, Btu/(lb)(°R)

T temperature, $^{\circ}\text{R}$
T* temperature used in determining losses, $T^* \Delta s = L$, $^{\circ}\text{R}$
V absolute velocity of gas, ft/sec
 α angle of absolute velocity, measured from tangential direction, deg
 γ ratio of specific heats
 Δ prefix indicating change
 φ circumferential position
 ρ gas density, lb/cu ft

Subscripts:

adj adjusted
p profile
R rotor
S stator
T tip
u tangential
x axial
O NACA standard sea-level conditions
1,2,3 measuring stations in turbine

Superscripts:

' stagnation state

APPARATUS AND INSTRUMENTATION

Summary of Blade Design

A conservatively designed single-stage turbine of free-vortex design was used in this investigation; it had low rotor-inlet relative Mach numbers, low turning angles, and high reaction at the rotor-root

section. The low hub-tip radius ratio (0.6) and zero tangential component of exit velocity make this design suitable for the last stage of a multistage turbine. The mean-section solidity of the 44-blade rotor was 1.56, based on the axial chord. The design specifications and conditions for the turbine are presented in reference 1, which also includes the velocity diagrams and a discussion of the blade-profile designs.

Turbine Installation

Dry air at a temperature of approximately 80° F and a pressure of about 25 pounds per square inch absolute was first passed through a filter tank to remove any foreign material present and was then ducted to the turbine plenum chamber. After passing through the turbine, the air was exhausted to the laboratory altitude-exhaust system. The power output of the turbine was absorbed by an electric dynamometer.

Instrumentation

A schematic cross section of the turbine installation showing measuring stations is presented in figure 1. Inlet conditions at station 1 were determined by three stagnation-pressure probes and three stagnation thermocouples.

A radial stagnation-pressure survey made at a point 1 inch upstream of the stator leading edge showed almost complete recovery of the stagnation pressure measured at station 1 except for relatively thin boundary layers at the inner and the outer walls. Similarly, surveys of the flow angle showed no whirl existing at the entrance to the stator-blade row.

Flow conditions at the stator and the rotor exits, stations 2 and 3, respectively, were obtained by the use of a circumferential survey mechanism indicated in figure 2. This mechanism consisted of a complete circumferential ring with three mounting pads at station 2, 0.25 inch downstream of the stator trailing edge, and three mounting pads 1 inch downstream of the rotor trailing edge at station 3. The three pads were located 38° apart on the upper half of the casing. Probe actuators were mounted on these pads so that the probes could be remotely controlled to move to any radial position in the annulus and could be rotated about their axes to any flow angle in the air stream. The entire survey ring could be circumferentially rotated 30° by means of a remotely controlled worm and gear drive. In addition, a thin flush ring was recessed in the fixed outer casing and driven by the probe actuator bases. The ring contained four wall static-pressure taps equally spaced circumferentially at each station. The recessed ring also served to cover the six probe-actuator slots in the fixed casing.

The stagnation pressures at the exits of the stator and the rotor were measured with the center tube of a hook-type three-claw probe. The

static pressure at the stator exit was measured by a wedge-type static-pressure probe calibrated for Mach number and immersion effects. The static pressure at the walls of each station was measured by 16 wall taps, 12 located in the inner shroud and 4 located in the outer wall in the thin flush ring. The flow angle was obtained with both the three-claw probe and the wedge-type static-pressure probe. A shielded thermocouple calibrated for Mach number effects was used to measure the stagnation temperature at the rotor exit. The photograph in figure 3 shows the types of probe used in the flow surveys.

Air flow was measured with a submerged 11.75-inch-diameter flat-plate orifice installed in a 24-inch duct in conformance with the specifications in reference 3. Turbine speed was measured by an electric chronometric tachometer.

Accuracy of Measurement

The wedge-type static-pressure probe and the three-claw probe were calibrated for Mach number and immersion effects in an annular tunnel having the same dimensions as the turbine annulus. The shielded thermocouple was calibrated in a variable-density jet over the same range of Mach numbers encountered in the flow investigation. The outer wall of the calibrating tunnel was fitted with a probe-actuator mounting pad identical with the pads on the circumferential survey ring. This mounting, which permitted the probes to be axially aligned with the flow in the tunnel and installed directly in the survey ring, eliminated any transfer errors in probe alignment.

In order to establish that the outside claws of the three-claw probe were not interfering with the pressure measurements in the regions of fluctuating flow downstream of the rotor, check surveys were made with a single-claw total-pressure probe. The probe was aligned with the flow by adjusting it until a maximum reading was obtained. It was found that identical results were obtained, so the three-claw probe was used exclusively thereafter. The velocity gradients in the stator-blade wakes caused the three-claw probes to be slightly misaligned with the flow direction in the blade-wake regions. However, the effect of this misalignment on the probe recovery coefficient is negligible.

The integrated weight flow at station 2 checked the orifice-measured weight flow within 1.0 percent. The discrepancy between the integrated weight flow at station 3 and the orifice-measured weight flow was 2.0 percent. The difference between integrated and orifice-measured weight flows at station 2 was probably due to circumferential variations and unsteady flows. The comparatively large discrepancy between integrated and orifice-measured weight flows at station 3 downstream of the rotating blades was caused primarily by the fluctuating flow existing downstream of the rotor blades. The value of the velocity obtained from converting the total pressure measured downstream of the rotor was somewhat larger

than the mass-averaged value because of the characteristics of the total-pressure probe in the fluctuating flow. As a result, all the velocities measured downstream of the rotor were somewhat high, and the survey results at this station should therefore be considered only qualitatively. The results are primarily valuable in indicating radial variations of the flow conditions at the exit of the rotor.

EXPERIMENTAL PROCEDURE

Surveys were made downstream of the stator and the rotor. Rotor and stator surveys were not carried out simultaneously, because wakes caused by the instruments downstream of the stator would affect instrument readings downstream of the rotor. The rotor was surveyed at approximately design stagnation pressure ratio and speed. The stator was surveyed with the rotor removed from the casing. The weight flow for the stator survey was set to correspond to that of the orifice-measured weight flow of the rotor survey. The design values of corrected equivalent weight flow and stagnation pressure ratio are compared with the values measured at the rotor as follows:

	$\frac{w\sqrt{\theta}}{\delta}$	$\frac{p_3'}{p_1'}$
Design	16.6	1.75
Survey	17.3	1.80

Circumferential surveys were taken downstream of the stator at 16 radial positions. Each circumferential survey covered slightly more than one blade passage and was complete enough to define the wake regions. Both static and stagnation pressures were determined.

Radial surveys were made at several circumferential positions downstream of the rotor. Circumferential variations were found to exist downstream of the rotor because of the stator wakes that persisted through the rotor. In figure 4, which is a plot of stagnation pressure ratio $\frac{p_3'}{p_1'}$ against circumferential position, the wakes are shown to occur approximately every 9° , which is the angular spacing of 40 stator blades. Circumferential surveys were therefore made at several radial positions in order to determine average values at each radius. Stagnation pressure, stagnation temperature, and flow angle were determined.

CALCULATION OF SURVEY DATA

Stator Surveys

In order to determine the radial variations of pressures, values obtained from circumferential surveys were mass-averaged according to the following equation over one blade spacing at each radius surveyed:

$$\frac{p_2'}{p_1'} = \frac{\int \frac{p_2'}{p_1'} \left(\frac{\rho V_x}{\rho' a_{cr}} \right)_2 d\phi}{\int \left(\frac{\rho V_x}{\rho' a_{cr}} \right)_2 d\phi}$$

Rotor Surveys

Circumferential averages of stagnation pressure, temperature, and flow angle at several radial points were used in conjunction with radial surveys in order to determine the radial variations of stagnation pressure, temperature, and angle. The static pressure was assumed to vary linearly between the averaged values obtained from the inner-wall and the outer-wall taps. The local efficiency was computed from the exit stagnation temperatures and pressures obtained from surveys and the entrance stagnation temperature and pressure.

Losses

The losses were divided between the stator and the rotor in proportion to the entropy rise in each. The rise in entropy across the turbine at each radius was determined from the local measured values of entrance and exit stagnation pressures and temperatures. The loss through the turbine was then determined by subtracting the actual enthalpy change from the ideal enthalpy change at each radial station. A temperature T^* was then determined such that the entropy rise multiplied by T^* would equal the total loss. The loss in the stator and that in the rotor at each radial station were determined by multiplying the local entropy rise in each by T^* . The equations for calculating the loss in this manner are given in the appendix.

RESULTS AND DISCUSSION

Surveys of the flow conditions and of the losses were made downstream of both the stator and the rotor of the turbine investigated. In addition, an analysis of the over-all measured losses was made in order to approximate the various components of loss.

Stator Losses

The losses at the exit of the stator are shown in the form of contour plots of the pressure-loss parameter $\frac{P_2' - P_2}{P_1' - P_2}$ in figure 5. High-loss cores caused by secondary flows exist at both the hub and the tip. In reference 4, photographs of smoke traces are presented which show the flow of the boundary-layer air along the upper and lower walls of a two-dimensional cascade toward the suction surface of the blade to form low-velocity cores of flow displaced radially inward from the hub and the tip similar to those observed in this investigation.

By circumferentially mass-averaging the stagnation pressure ratio $\frac{P_2'}{P_1'}$ over one-blade spacing for each radius surveyed, a radial distribution of this ratio can be determined. In figure 6, this ratio $\frac{P_2'}{P_1'}$ is plotted against radius. The total-pressure drop near the hub of the stator is somewhat greater than that near the tip. The loss in total pressure over the center portion of the blade is nearly negligible.

Measured Flow Conditions Downstream of Rotor

The results of the surveys of the flow conditions downstream of the rotor are presented in figures 7 through 9.

The radial variations of flow angle at the exit of the rotor are presented in figure 7. The flow is seen to be underturned from the design value over the lower part of the blade height, overturned over part of the upper half of the blade, and underturned at the tip. The variation in flow angle near the hub is evidently caused by secondary-flow phenomena which evidently tend to increase the underturning a short distance away from the inner wall.

The radial variation of the circumferentially averaged values of the absolute critical velocity ratio $\left(\frac{V}{a_{cr}}\right)_3$ and the axial and tangential components corresponding to the measured flow angles over the blade height are shown in figure 8. The underturning near the rotor hub caused positive values of the tangential velocity in this region. The dips in the axial-velocity distribution at radii of about 4.7 and 6.7 inches near the hub and the tip, respectively, are evidently the result of low-velocity cores of vortices caused by secondary flows similar to those observed downstream of the stator. The tangential velocity at the rotor exit is so small that the corresponding loss in available work output is practically negligible.

The radial variation of the specific mass-flow parameter $\frac{(\rho V_x)_3}{(\rho' a_{cr})_1}$ is presented in figure 9. The trends of this curve closely follow those of the axial-velocity component.

Measured Losses Downstream of Rotor

The radial variations of the loss - mass-flow parameters are presented in figure 10. The dashed line represents the stator loss multiplied by a mass-flow parameter $L_S \frac{r}{r_T} \frac{(\rho V_x)_2}{(\rho' a_{cr})_1}$.

Values of the rotor-loss - mass-flow parameter $L_R \frac{r}{r_T} \frac{(\rho V_x)_3}{(\rho' a_{cr})_1}$ are added to the stator-loss - mass-flow parameter to obtain the solid curve in figure 10. The value of the measured rotor-loss - mass-flow parameter is small compared with the over-all loss measured in the performance study because of the inherent errors in measurements downstream of the rotating blades.

In order to obtain rotor-survey data which would agree with the over-all efficiency measured in the turbine-performance study, the measured rotor-loss - mass-flow parameter was adjusted so that the sum of the integrated rotor loss from the adjusted survey data plus the integrated stator loss was equal to the loss measured from the performance investigation at the design point of operation. A radially constant correction was added to the rotor-loss - mass-flow parameter $L_R \frac{r}{r_T} \frac{(\rho V_x)_3}{(\rho' a_{cr})_1}$ to obtain parameter $L_{R,adj} \frac{r}{r_T} \frac{(\rho V_x)_3}{(\rho' a_{cr})_1}$. The adjusted parameter was added to the stator-loss - mass-flow parameter to obtain the upper curve in figure 10. Even though the addition of a radially constant correction is arbitrary and probably is not exact, the over-all correction is sufficiently small that the loss distribution would not be appreciably changed regardless of the correction distribution used.

Comparison of the stator-loss - mass-flow parameter with the adjusted total-loss - mass-flow parameter indicates that the rotor losses constitute the major part of the over-all losses.

It is evident from figure 10 that the greater portion of the loss occurs over the inner and the outer portions of the blade span; whereas, the loss over the center portion of the blade is comparatively small.

The losses over the outer portion of the blade near the tip section are considerably greater than those near the hub section. Any substantial increase in over-all efficiency must be obtained by improved flow through the rotor-blade passages near the hub and the tip.

Analysis of Stator and Rotor Losses

A method for estimating the various losses in a turbine is given in reference 2. The evaluation of the profile losses is based on stationary-cascade data. The difference between the total loss and the profile loss is defined as the sum of the secondary-flow and tip-clearance losses. An empirical method for estimating the secondary-flow and the tip-clearance losses is also given. The method, which is based on stationary-cascade and turbine rotor data, may be used to predict an average secondary and tip-clearance loss based on the blade profile and the flow angles at the mean radius.

By use of reference 2, profile losses were computed for the root and the mean sections of both the stator and the rotor and also for the tip section of the stator. Because the method does not extend to profiles such as those of the rotor-tip section, reference 5 was used in determining the profile loss for that section. Although the data in reference 5 are for decelerating compressor blading, the drag coefficient obtained for the tip section agrees well with extrapolated values of the profile-loss coefficient obtained for the hub and mean blade sections from reference 2. The losses determined from these references are expressed as loss coefficients in the form of the ratio of the drop in total pressure across a blade row to the exit dynamic pressure. A total-loss coefficient was calculated from the measured survey data. Profile-loss coefficients for both the stator and the rotor were determined from the data given in references 2 and 5 which are based on two-dimensional cascade studies. The total-loss parameter L was then multiplied by the ratio of the profile-loss coefficient to the total-loss coefficient in order to obtain the profile-loss parameter L_p for each blade row. An indication of the secondary-flow and the tip-clearance losses is obtained by subtracting the calculated profile loss from the measured total loss. A value for the tip-clearance loss for the rotor was calculated by using the formula given in reference 2.

The measured stator total-loss - mass-flow parameter $L_S \frac{r}{r_T} \frac{(\rho V_x)_2}{(\rho' a_{cr})_1}$ obtained from surveys and the calculated profile-loss - mass-flow parameter $L_{S,p} \frac{r}{r_T} \frac{(\rho V_x)_2}{(\rho' a_{cr})_1}$ are plotted against radius in figure 11(a).

Over the center portion of the blade, the calculated profile loss is roughly twice the measured total loss. Evidently, the stator blades of

the turbine investigated herein have considerably less profile loss than those investigated in cascade and reported in reference 2. The measured loss over the center portion of the blade is essentially constant and constitutes the level of the actual profile loss. The increased losses at the hub and the tip sections are caused by the additional shroud boundary layers and the secondary flows at the blade extremities.

A breakdown of the rotor losses is presented in figure 11(b). The adjusted rotor-loss - mass-flow parameter obtained from surveys

$$L_{R,adj} \frac{r}{r_T} \frac{(\rho V_x)_3}{(\rho' a_{cr})_1} \quad \text{and the calculated profile-loss - mass-flow parameter}$$

$$L_{R,p} \frac{r}{r_T} \frac{(\rho V_x)_3}{(\rho' a_{cr})_1} \quad \text{are plotted against radius. The area representing tip-}$$

clearance loss is proportional to the value of the loss calculated on the basis of information presented in reference 2 and is arbitrarily distributed over the tip section of the blade as shown.

For the rotor, the calculated profile loss agrees more reasonably with the adjusted total loss than it did for the stator. The profile loss is less than the adjusted total rotor loss over the entire blade height, except at a radius of 5.2 inches where the two losses are equal. The value of the profile loss, mass-averaged over the entire blade height, is 31 percent of the value of the adjusted total rotor loss. The calculated tip-clearance loss is 9 percent of the total rotor loss. The remaining 60 percent of the loss can be attributed to secondary flows. The secondary-flow loss determined in this manner is about twice as large as the secondary-flow loss predicted in figure 17 of reference 2.

SUMMARY OF RESULTS

Surveys of the flow conditions and of the losses at the exit of both the stator and the rotor of a conservatively designed turbine suitable for the last stage of a multistage turbine were made in order to determine the radial variations of the flow and the losses within the turbine. The following results were obtained:

1. The major losses in the turbine were in the rotor near the blade extremities (hub and tip). The losses near the tip of the blade were considerably greater than those near the hub.

2. The surveys of the stator indicated that the losses over the center portion of this blade row were nearly negligible. Comparison of the stator-loss - mass-flow parameter with the adjusted total-loss - mass-flow parameter indicated that the rotor losses constituted the major part of the over-all losses.

3. Surveys at the exit of both the stator and the rotor showed low-velocity cores near both the hub and the tip sections that indicated the existence of secondary flows.

4. The rotor profile loss and the tip-clearance loss as calculated with an empirical method are 31 and 9 percent of the adjusted total measured rotor loss, respectively. The remaining 60 percent of the loss was attributed to secondary flows.

Lewis Flight Propulsion Laboratory
National Advisory Committee for Aeronautics
Cleveland, Ohio

2560

APPENDIX - METHOD FOR CALCULATING OVER-ALL TURBINE LOSS
BETWEEN STATOR AND ROTOR

The over-all turbine loss is divided between the stator and rotor in proportion to the entropy rise in each. The over-all loss L_{1-3} at any radius may be calculated from the survey total-pressure and temperature measurements at the rotor exit:

$$L_{1-3} = c_p T_{1'} \left[\frac{T_{3'}}{T_{1'}} - \left(\frac{p_{3'}}{p_{1'}} \right)^{\frac{\gamma-1}{\gamma}} \right] \quad (A1)$$

The entropy rise across the stator is

$$\Delta s_{1-2} = s_2 - s_1 = - \frac{R}{J} \ln \frac{p_{2'}}{p_{1'}} \quad (A2)$$

The over-all entropy rise across the turbine is

$$\Delta s_{1-3} = s_3 - s_1 = c_p \ln \frac{T_{3'}}{T_{1'}} - \frac{R}{J} \ln \frac{p_{3'}}{p_{1'}} \quad (A3)$$

As shown in the temperature-entropy diagram of figure 12, a temperature T^* may be defined such that

$$\left. \begin{aligned} T^* \Delta s_{1-3} &= T^* (s_3 - s_1) = L_{1-3} \\ \text{or} \quad T^* &= \frac{L_{1-3}}{\Delta s_{1-3}} \end{aligned} \right\} \quad (A4)$$

After T^* is obtained from equation (A4), the individual stator and rotor losses at any radius may be calculated from the following relations:

$$\left. \begin{aligned} L_{1-2} &= T^* \Delta s_{1-2} \\ L_{2-3} &= L_{1-3} - L_{1-2} \end{aligned} \right\} \quad (A5)$$

REFERENCES

1. Heller, Jack A., Whitney, Rose L., and Cavicchi, Richard H.: Experimental Investigation of a Conservatively Designed Turbine at Four Rotor-Blade Solidities. NACA RM E52C17, 1952.
2. Ainley, D. G., and Mathieson, G. C. R.: An Examination of the Flow and Pressure Losses in Blade Rows of Axial Flow Turbines. Rep. No. R. 86, British N.G.T.E., March, 1951.
3. Anon.: Fluid Meters, Their Theory and Applications. A.S.M.E. Res. Pub., Am. Soc. Mech. Eng. (New York), 4th ed., 1937.
4. Herzig, H. Z., Hansen, A. G., and Costello, G. R.: Visualization of Secondary-Flow Phenomena in Blade Row. NACA RM E52F19, 1952.
5. Herrig, L. Joseph, Emery, James C., and Erwin, John R.: Systematic Two-Dimensional Cascade Tests of NACA 65-Series Compressor Blades at Low Speeds. NACA RM L51G31, 1951.

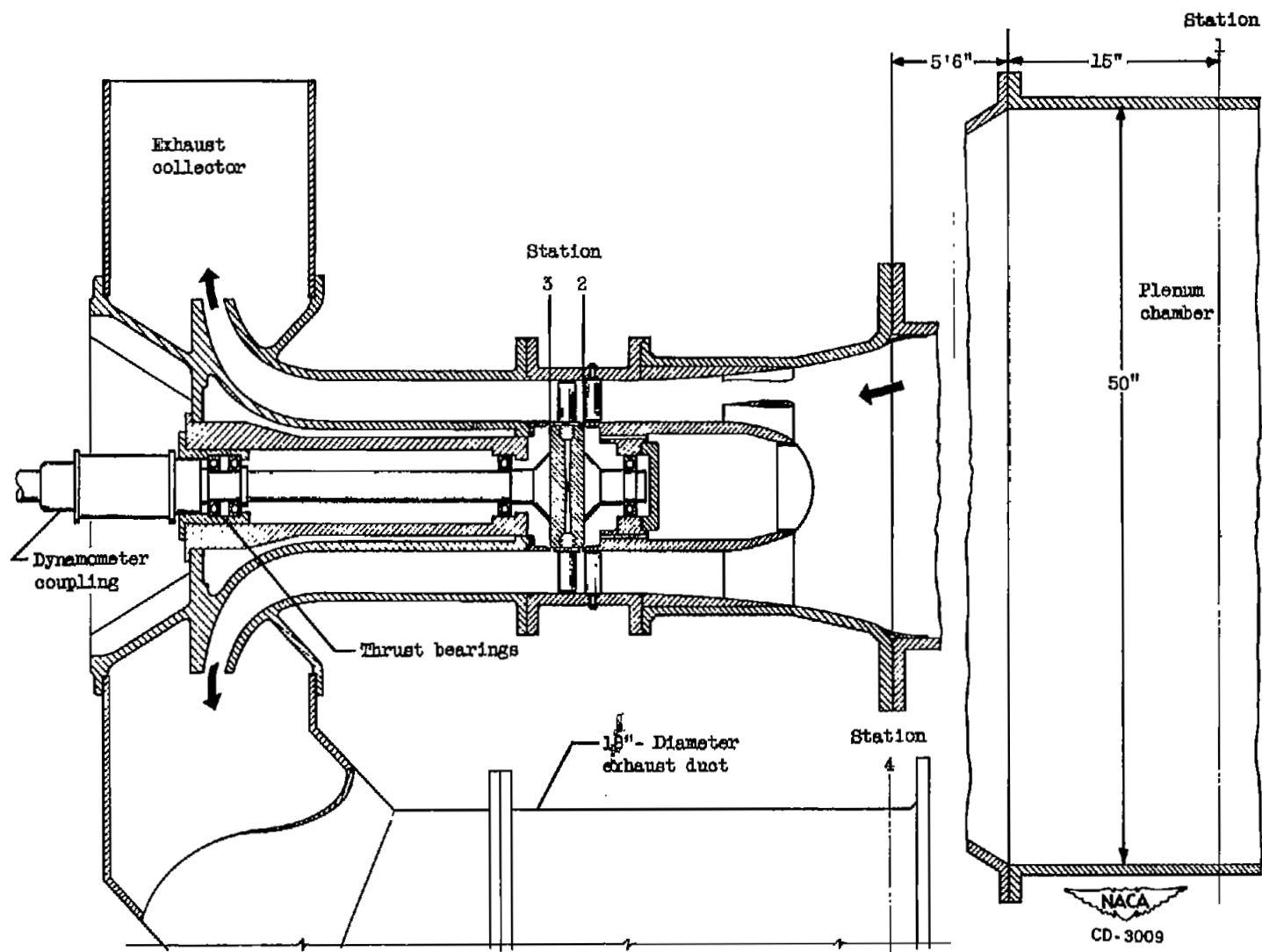


Figure 1. - Schematic diagram of turbine installation showing measuring stations.

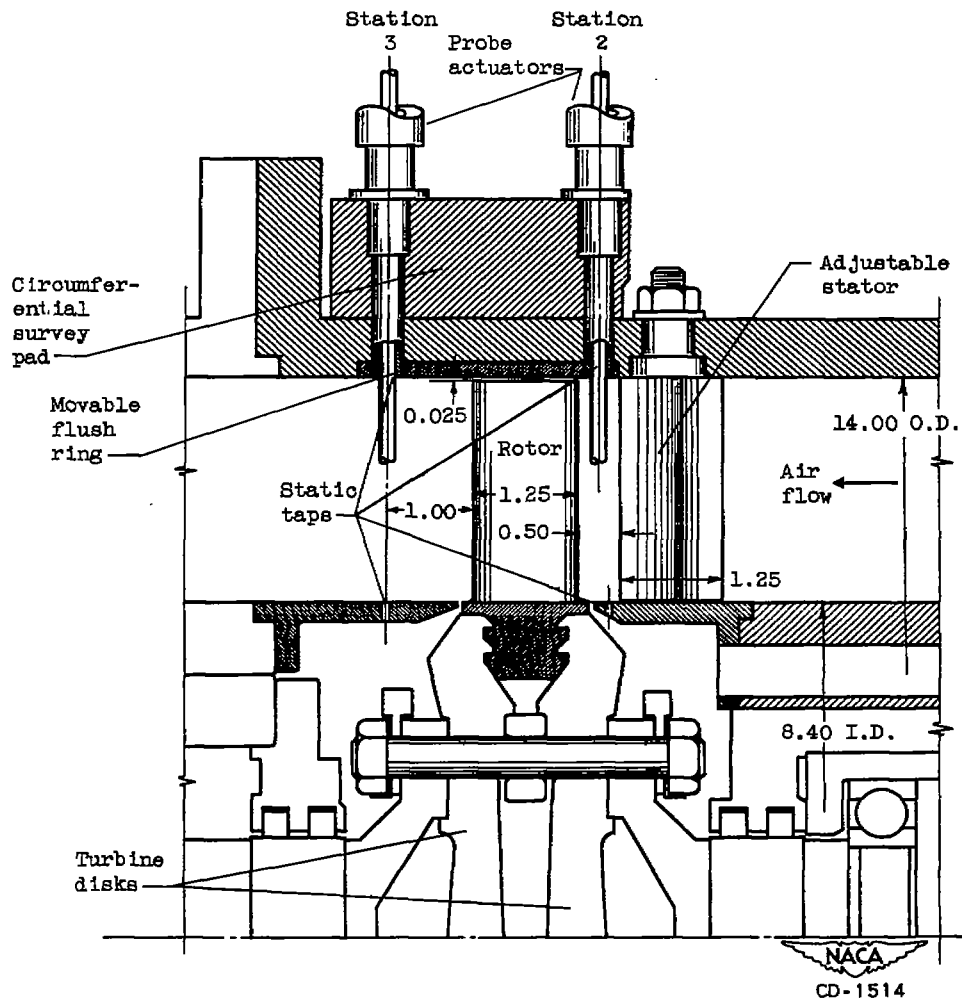


Figure 2. - Section of turbine showing blading and instrumentation. (All dimensions in inches.)

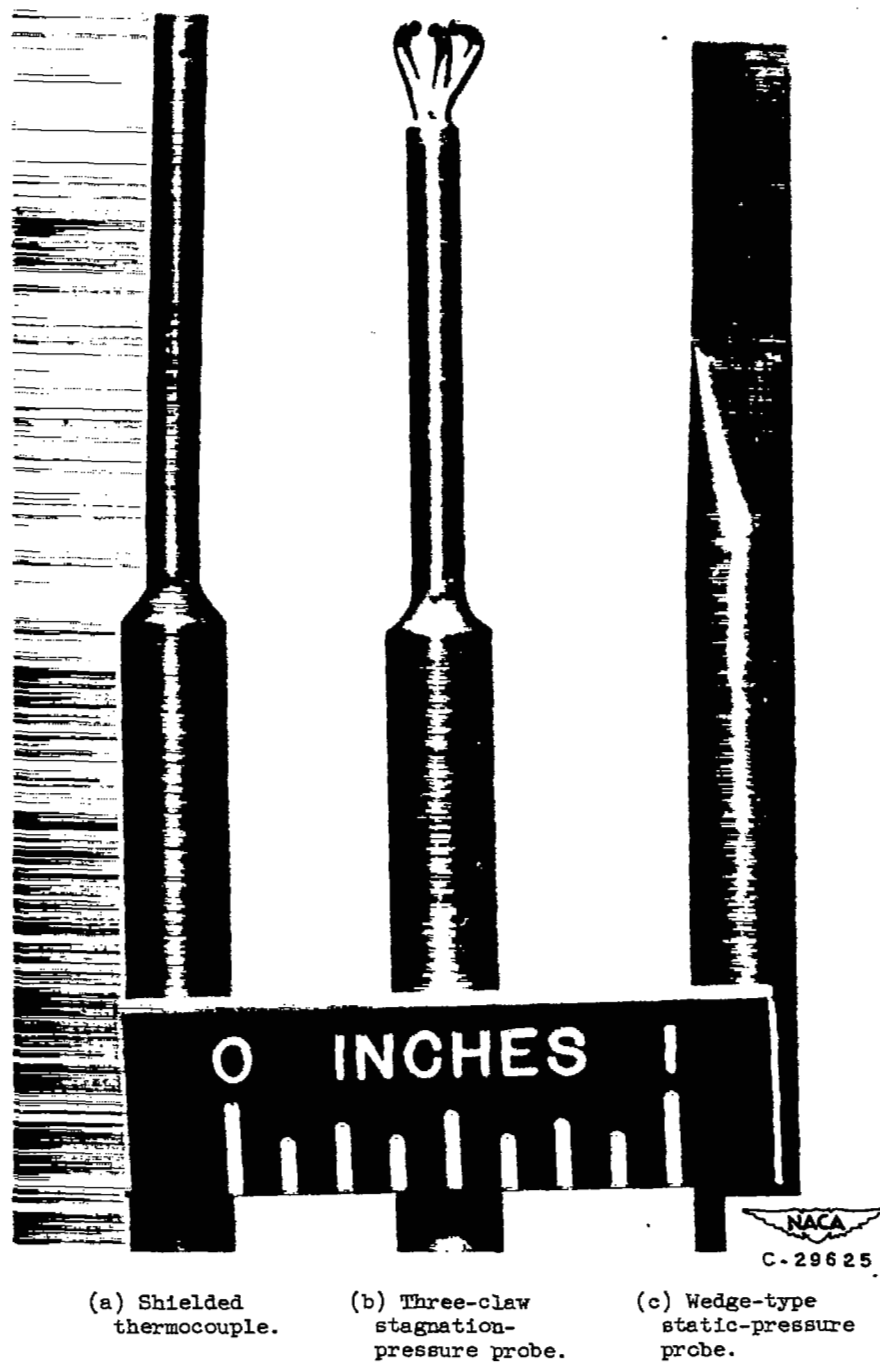


Figure 3. - Survey instruments.

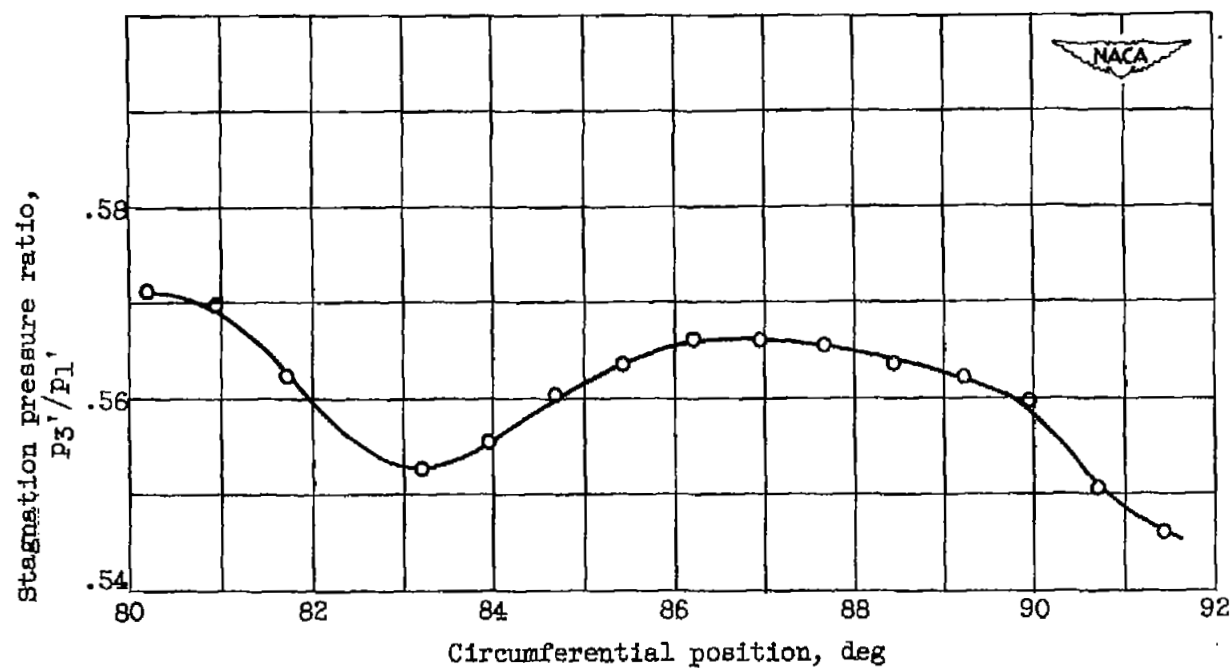


Figure 4. - Circumferential variation of stagnation pressure ratio at mean radius of rotor exit.

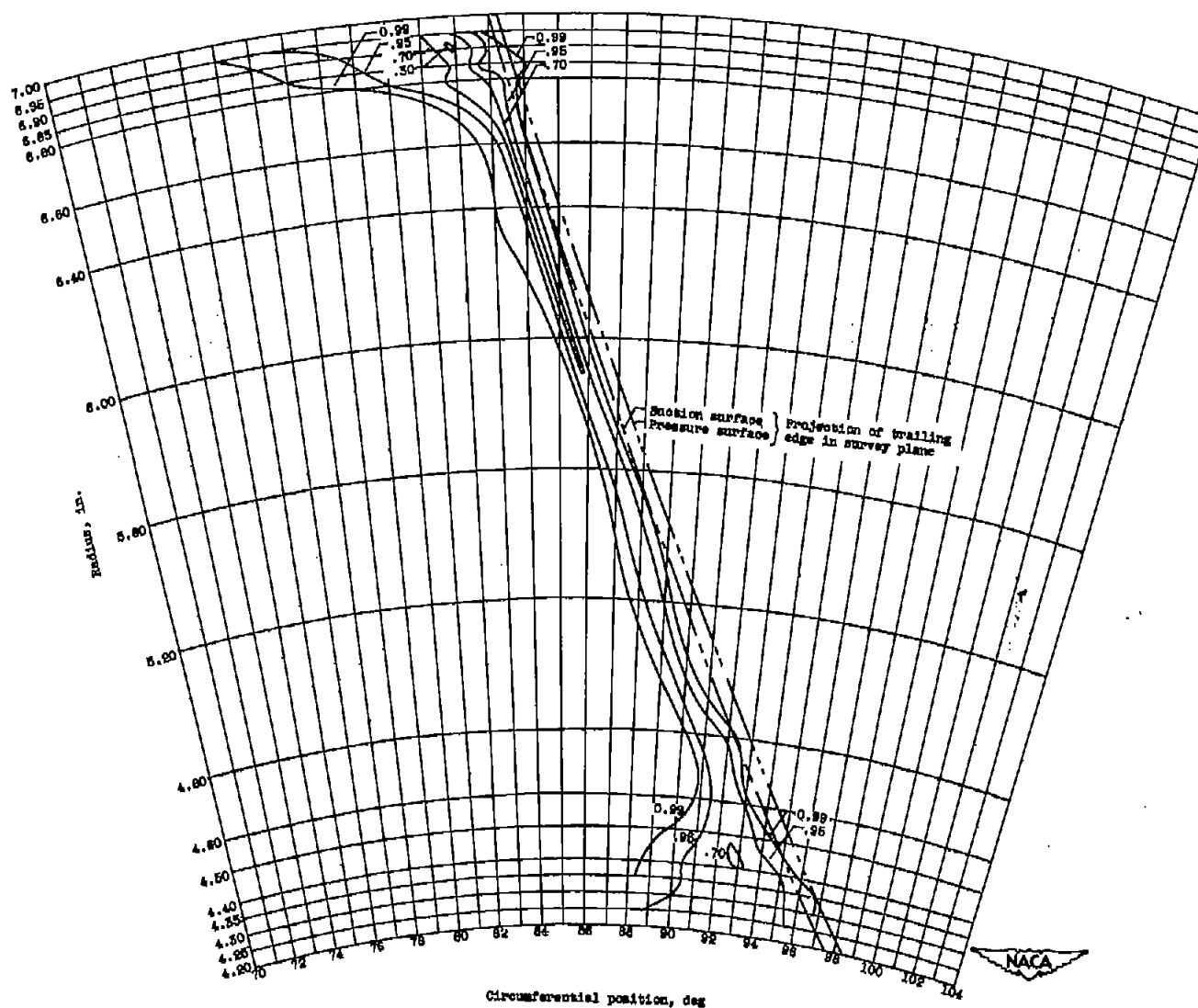


Figure 5. - Contours of pressure-loss parameter $\frac{P_2 - P_2}{P_1 - P_2}$ downstream of stator.

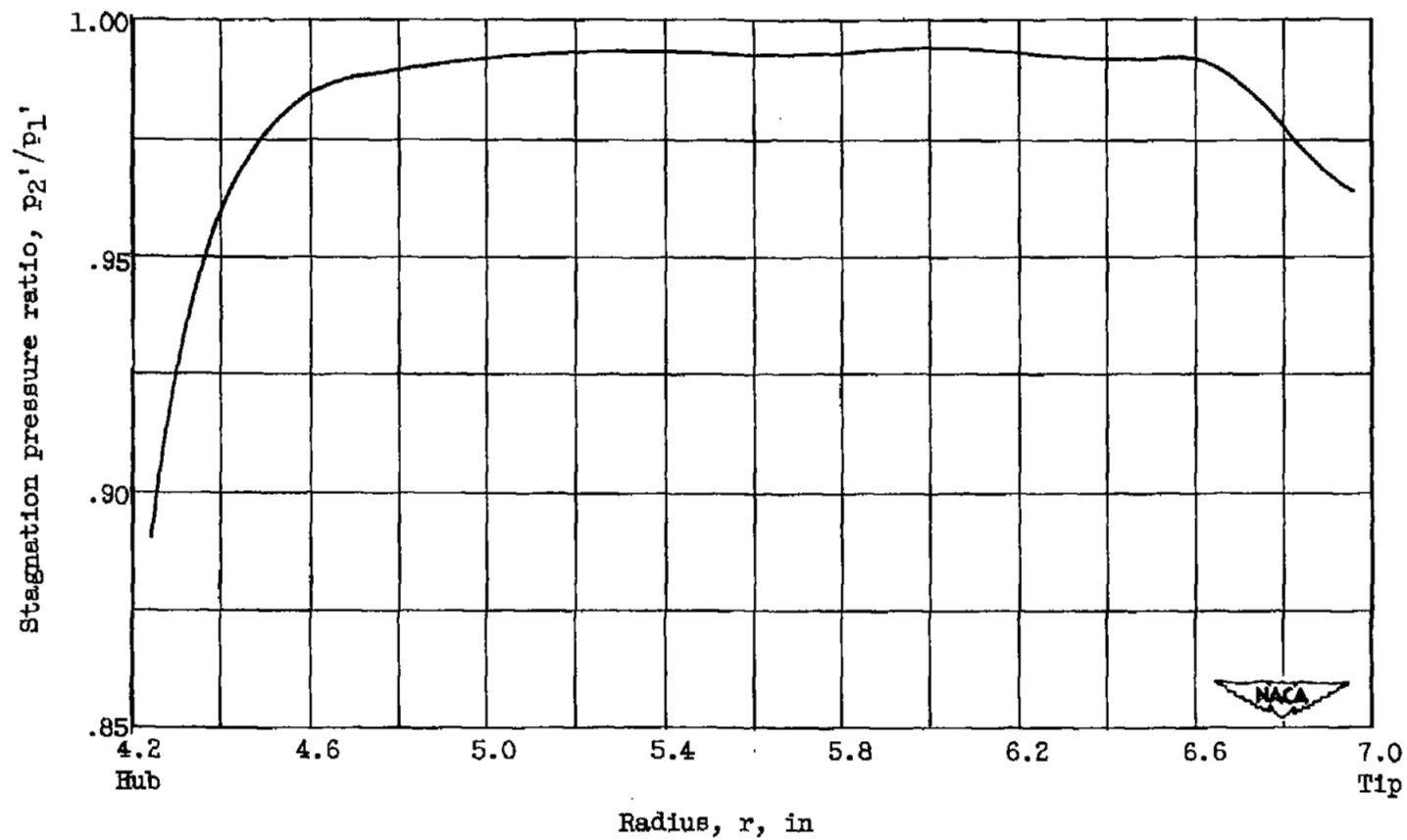


Figure 6. - Radial variation of stagnation pressure ratio at stator exit.

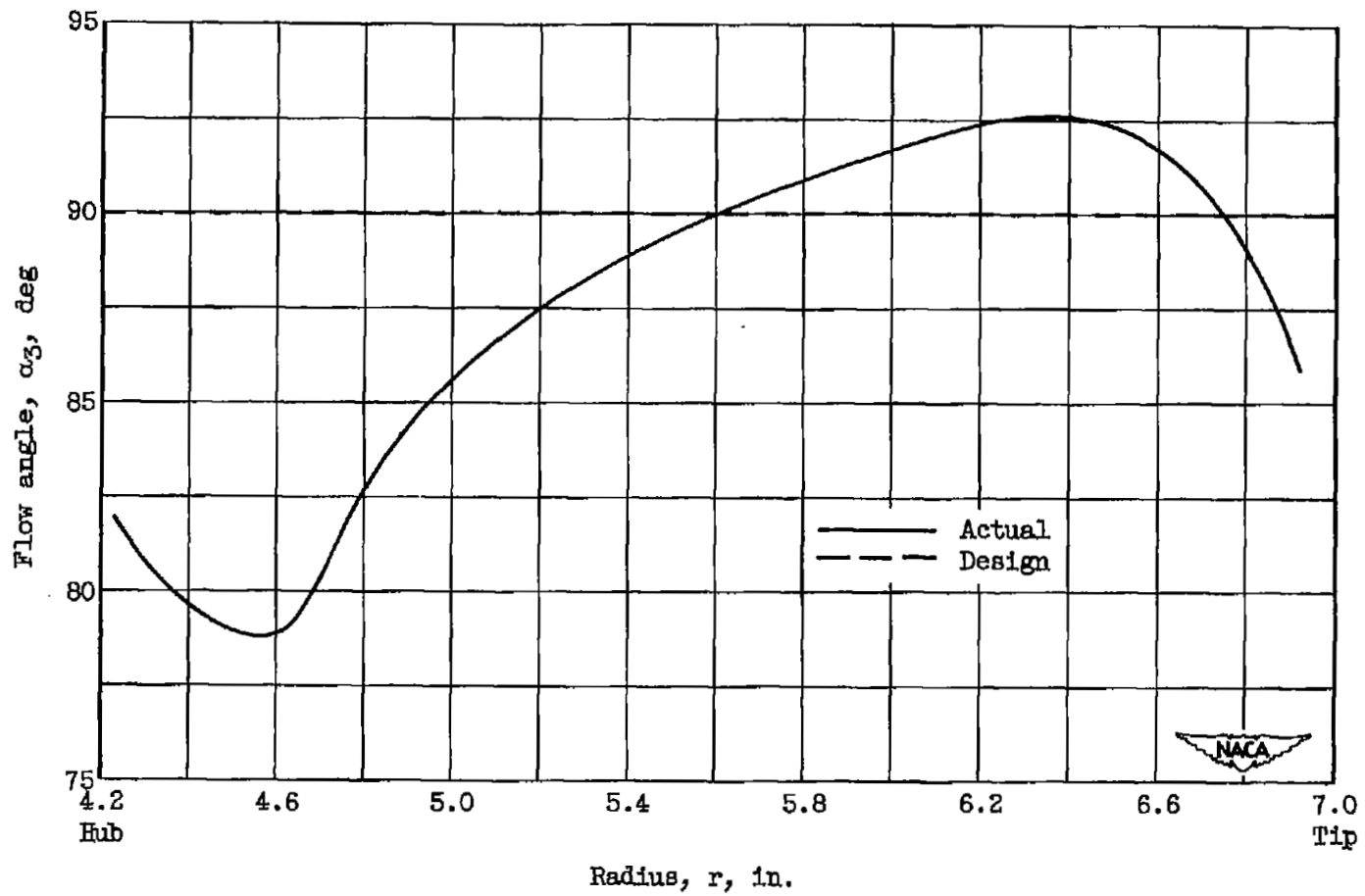


Figure 7. - Radial variation of flow angle at rotor exit.

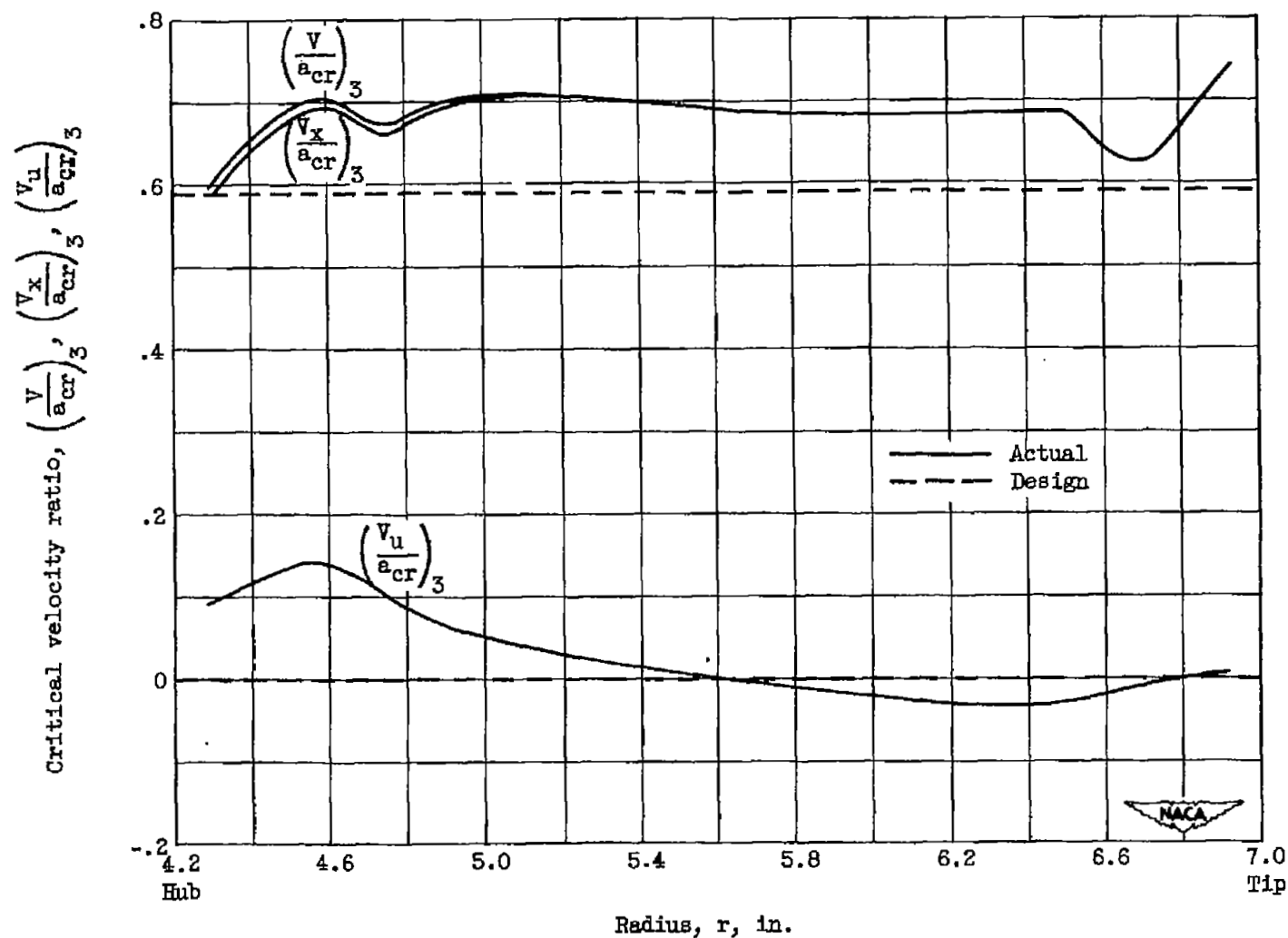


Figure 8. - Radial variation of critical velocity ratio, and axial and tangential components of critical velocity ratio at rotor exit.

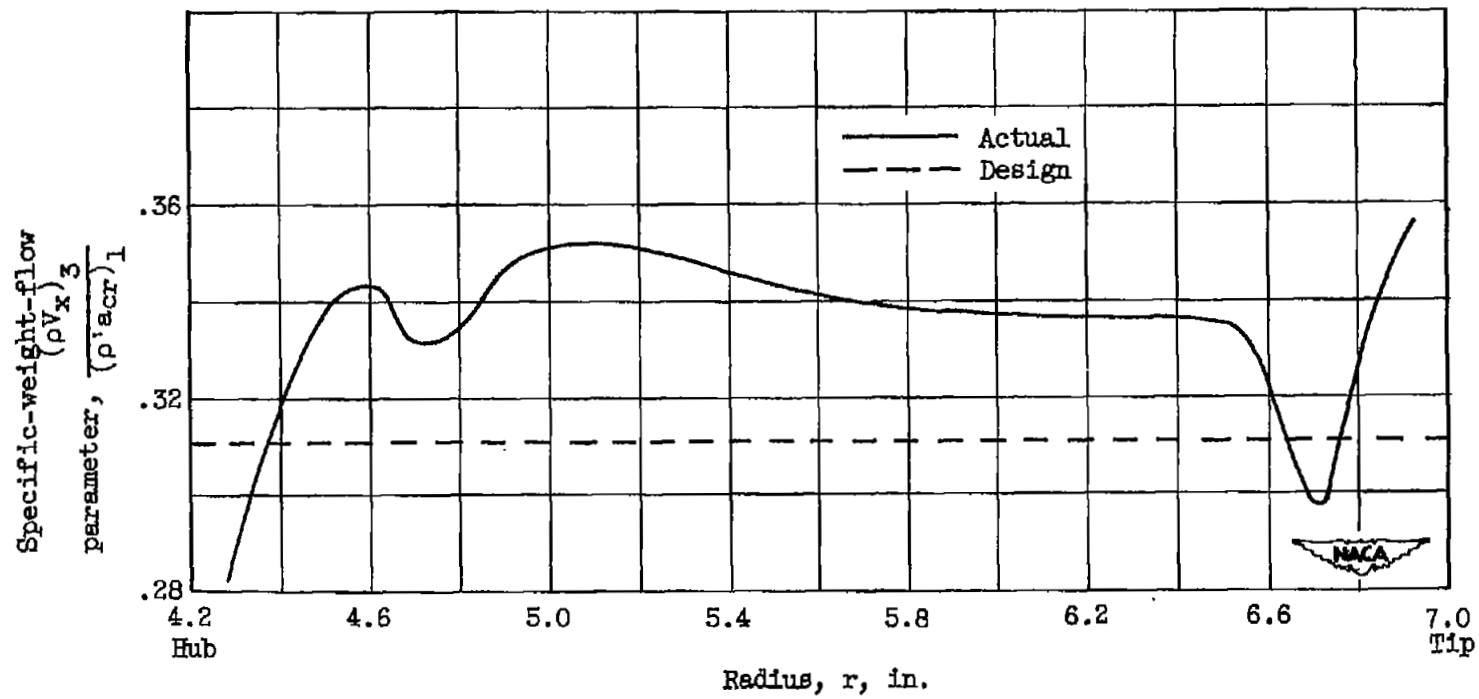


Figure 9. - Radial variation of specific-weight-flow parameter at rotor exit.

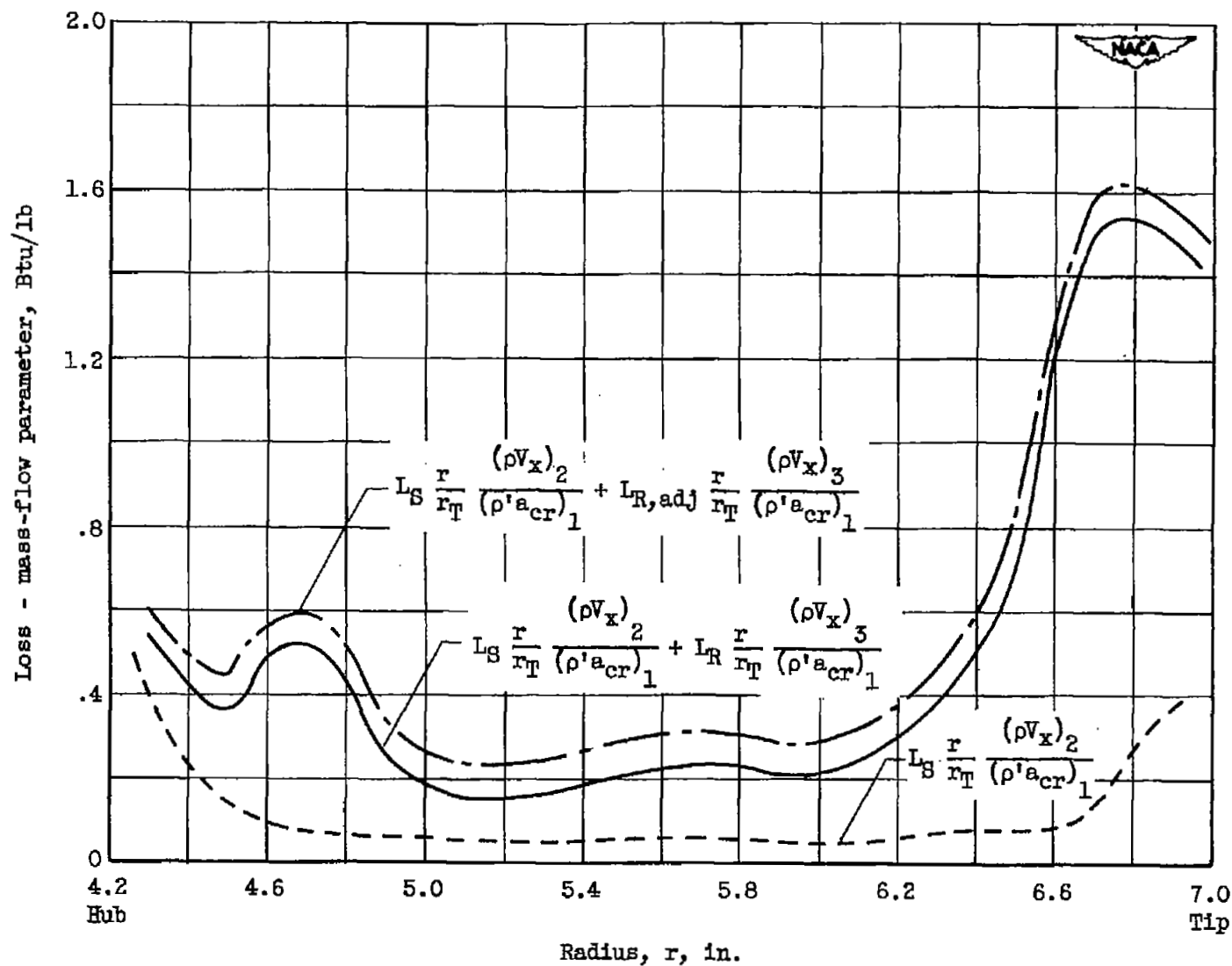


Figure 10. - Radial variation of loss - mass-flow parameter at exit of stator and rotor.

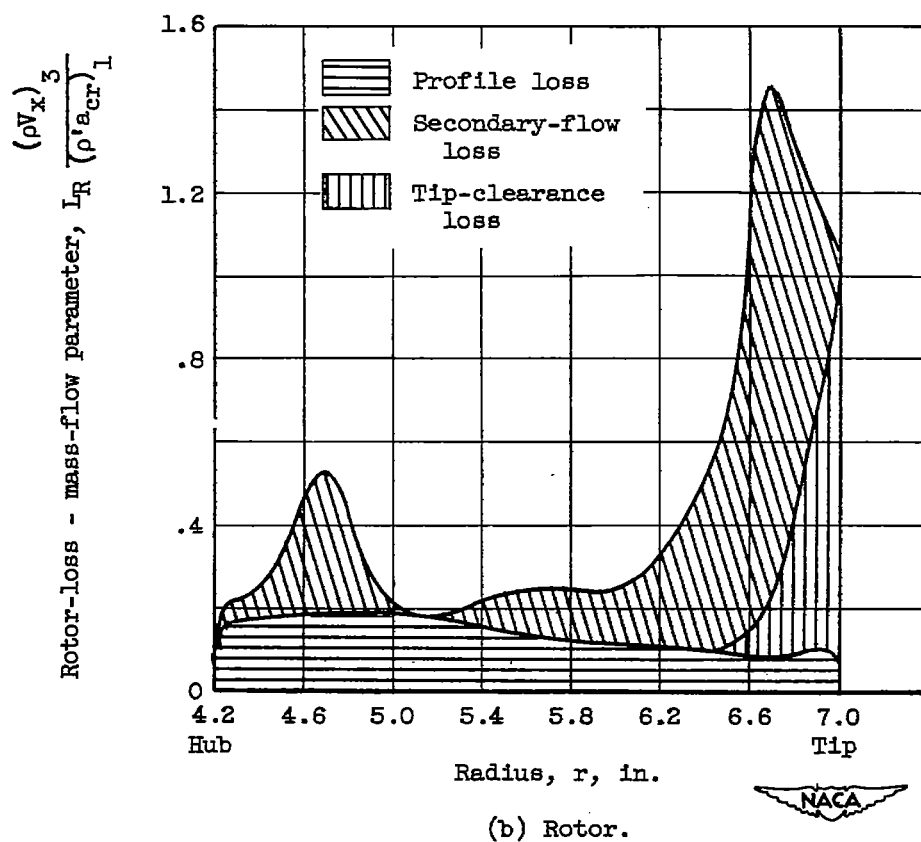
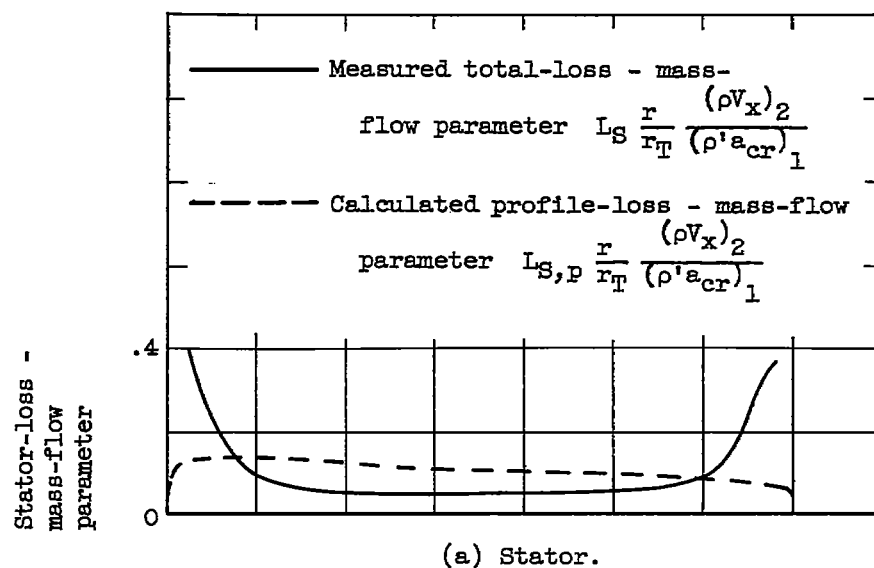


Figure 11. - Analysis of losses on basis of information presented in reference 2.

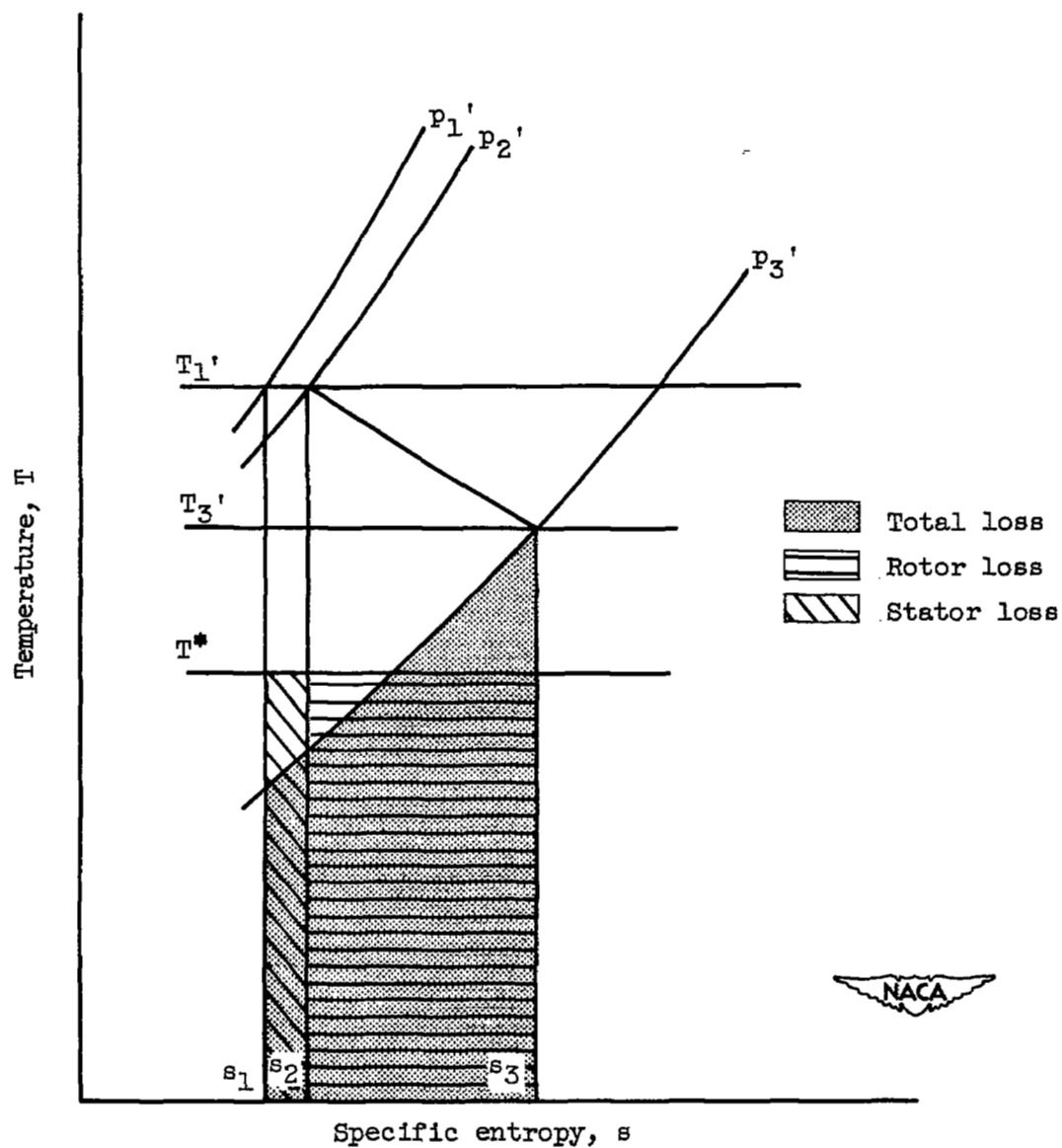


Figure 12. - Temperature-entropy diagram showing method for calculating losses for both stator and rotor.

SECURITY INFORMATION

[REDACTED]

□

NASA Technical Library



3 1176 01435 6720



[REDACTED]